THE UNIVERSITY OF TENNESSEE KNOXVILLE

International Journal of Nuclear Security

Volume 7 | Number 1 Article 4

3-1-2021

Investigation of the use of Coincidences Between Fast Neutrons and Gamma Rays for the Detection of Special Nuclear Materials

Débora M. Trombetta
Royal Institute of Technology - KTH

Bo Cederwall
Royal Institute of Technology - KTH

Kåre Axell
Swedish Radiation Safety Authority - SSM

International Journal of Nuclear Security, Vol. 7, No. 1, 2021

Investigation on the Use of Coincidences Between Fast Neutrons and Gamma Rays for the detection of Special Nuclear Materials

Débora M. Trombetta[1], Bo Cederwall[1], and Kåre Axell[2]
[1]Royal Institute of Technology – KTH
[2]Swedish Radiation Safety Authority – SSM

Abstract

The emergence of new methodologies with promising applications that could impact nuclear security and emergency preparedness detection systems in the near future motivate the development of computational tools that allow the theoretical investigation of the relevant design parameters for such detection systems. Here, we present Monte Carlo simulations using the MCNP6 code to investigate the use of fast neutron-neutron and gamma-neutron coincidences in addition to conventional methods for detection of special nuclear materials (SNM) using inorganic scintillator detectors. The results show fair agreement between MCNP6 and MCNP-PoliMi simulations for neutron-neutron coincidences and that coincident detection of gamma rays and fast neutrons has a potential for enhancing the sensitivity for detection of SNM compared with conventional gamma-ray, single-neutron, and fast neutron-neutron coincidence detection schemes.

Keywords: organic scintillator detector, Monte Carlo simulations, MCNP, nuclear security, special nuclear materials

I. Introduction

Nuclear and radioactive materials outside of regulatory control (MORC) are detected with radiation detection systems, such as Radiation Portal Monitors (RPM). The use of organic scintillators for neutron detection in such applications **[*1*–*5*]** is a new technology that has gained attention in recent years. In 2011, the International Atomic Energy Agency (IAEA) addressed the possible future shortage of helium-3 by encouraging investigation of new neutron detection systems replacing the helium-3-based neutron detectors **[*6*]** currently used, leading to an enhanced focus on such developments. However, gas-filled

doi:10.7290/ijns070104

International Journal of Nuclear Security, Vol. 7, No. 1, 2021

proportional counters based on helium-3 still remain the most commonly used detectors in nuclear security systems **[*7, 8*]**.

Organic Scintillators with fast timing and pulse shape discrimination capabilities enable efficient detection and identification of gamma rays and neutrons **[*2, 9*]**. The use of this type of detectors may result in a higher sensitivity for detecting special nuclear materials, since nuclear fission is associated with the emission of neutrons and "cascades" of gamma rays depopulating excited states in the fission products. Most of these gamma rays are "prompt," i.e. emanate from short-lived nuclear states, and their multiplicity distribution can be extended significantly beyond an average of 5-10 **[*10–12*]**. The use of particle coincidences has been extensively used in the quantitative analysis of samples with respect to their content of SNM. A priori, the use of gamma-gamma correlations is appealing due to the relatively high multiplicity of gamma rays as mentioned above. However, in the presence of strong background radiation from radioactive decay gamma rays the rate of accidental coincidences may be a concern. The strong attenuation of gamma rays in dense and large objects also needs to be considered, e.g. in nuclear safeguards applications. Therefore, neutron-neutron (nn) coincidence techniques are usually preferred **[*2, 5, 13–17*]** as they are also subject to low natural background rates, even though the spread in the correlation time for neutrons pairs is larger than for photons, due to the time-of-flight dependence on the neutron energy. Indeed, it has been shown **[*5*]** that a multidetector setup based on organic liquid scintillation detectors can be as efficient in detecting SNM as a high-end commercial system based on moderated helium-3 counters **[*18*]**. Another promising development is the use of fast gamma-neutron (gn) coincidence correlations between prompt neutrons and gamma rays in the quantification of fissile materials in nuclear safeguards and security applications **[*19*]**. Gamma-fast neutron coincidence detection may have a higher sensitivity as well as a higher specificity than fast nn coincidences for the detection of SNM due to high gamma-ray multiplicity and the unique time correlations between the photons and neutrons emitted in fission, respectively **[*17, 19, 20*]**.

A key issue for the design of detector systems for this purpose is the ability of a theory to accurately reproduce the particle and photon emission from fission and its implementation in state-of-the-art Monte Carlo codes **[*20*]**. Computational simulations can be used to study the design and key parameters of a system prior to prototype development, which is time and cost reducing, and may also improve the definitions of system performance criteria.

In a previous study **[*19*]**, the use of gn coincidence counting rates was proposed as a sensitive method for detection and quantification of SNM. This study presented a comparison between gamma- gamma, neutron-neutron, and gamma-neutron time correlations along with the respective simulations results. This paper continues the investigation of the use of gamma and fast neutron coincidences to detect nuclear materials using Monte Carlo simulations. Considering the possible applications of this technique, we present a sensitivity analysis of fast nn and gn coincidence counting rates with respect to the effective mass of the sample, as well as a comparison with literature results obtained with MCNP-PoliMi.

II. Method

In this work, version 6.2 of MCNP, which is a merge between MCNP5 and MCNPX, is used for the design study of an RPM application. The code includes fission multiplicity options and a new model applied for correlated prompt secondary particle production **[*21*]**. The spontaneous decay option that was implemented in MCNPX (2008) has been extended in version 6 to include spontaneous fission neutrons (PAR=SN), and the codes CGMF and FREYA **[*22*]**, which includes gamma ray multiplicity information for fission events.

doi:10.7290/ijns070104

International Journal of Nuclear Security, Vol. 7, No. 1, 2021

A. MCNP simulation details

To simulate the spontaneous fission source, the SDEF card was used with PAR=SF (Spontaneous Fission), and the fission model CGMF **[*22*]** was chosen in the FMULT card. The emitted neutrons and photons with their associated multiplicities are correlated with each fission event. MCNP samples the energy distribution from the two Watt-fission spectra parameters ***[21]***. Decay gamma production is included by the source option PAR=SP (Spontaneous Photons), based on the relative activities of the unstable isotopes in the material. The energy spectra for induced fission is chosen from parameters in the nuclear data tables of transport cross section.

The PTRAC card was used to create an output data file of user-filtered particle/cell events, recording information such as: type of event (collision, capture, termination or a banked event); time of a given event; momentum; and particle energy after a given event. In the literature **[*23, 24*]**, this card was previously used with the option for coincidence neutron capture and with the CAP option (neutron capture tally), that scores the number of captured neutrons in a specific combination of nuclides at the end of each history. In the present study, we tracked the particle scattering events and accessed the time between correlated neutrons and gammas from fission events and their deposited energy as predicted by the simulations.

A MATLAB™ **[*25*]** post processing code was created to organize the PTRAC output file in a table, filter the events, perform the coincidence counting, and calculate the correlation time and energy deposition. The script identifies scattering events for neutrons and gammas generated in the same fission event that occurred in different detectors within a coincidence time window of 200ns. Ref. **[*19*]** presents the validation of the computational model and method used for gamma-neutron and neutron-neutron coincidence counting.

III. Results

A. MCNP6 and MCNP-PoliMi

The Monte Carlo code MCNPX-PoliMi is commonly applied for such studies and has been developed from the MCNP code for special use in safeguards experiments that rely on the detection of prompt neutrons and gamma rays from fission **[*3, 5, 19, 20, 26*]**. One special feature of the MCNPX-PoliMi code is that it provides tallies on an event-by-event basis. An equivalent tally, used here, can be produced by MCNP6, and MCNPX, using the PTRAC card option.

The single neutron and neutron-neutron coincidence count rates for four different PuO2 samples were calculated with MCNP6 and compared with the experimental data and MCNP-PoliMi calculations presented in Ref. **[*5*]**. The experiment reported in Ref. **[*5*]** made use of four Eljen Technology EJ-309 liquid scintillation detectors **[*27*]**; two of 5”x 5 ”and two of 3”x 3 ”size. A time-synchronized 8- channel, 250 MHz CAEN VX1720 digitizer module was used to sample the pulse waveforms from the detectors during approximately 180 s per sample. It consisted of two concentric rings of eight, placed in a cylindrical geometry around the samples, using an aluminum holding structure with a cavity diameter of 34 cm. MCNP6 modelling setup is presented in Figure 1.

doi:10.7290/ijns070104

International Journal of Nuclear Security, Vol. 7, No. 1, 2021

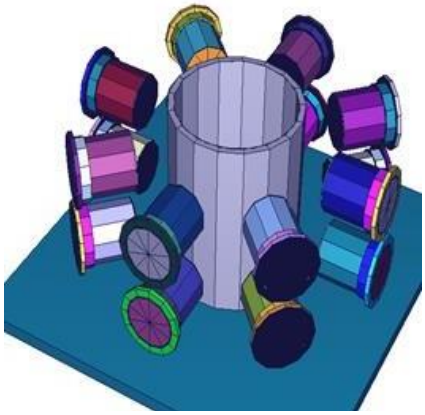

Figure 1: MCNP6 modeling of experimental setup [*5*]. The sample was placed at the center of the setup and surrounded by 1 cm lead shielding.

Figure 2 presents the neutron singles and nn coincidence rates as a function of the 240Pueff mass for the experimental data and the corresponding MCNPX PoliMi simulations taken from Ref. **[*5*]** along with the MCNP6 simulations performed in the present work. All error bars for simulation results are added in the plots, although sometimes not visible since it was smaller than the data point in some cases. The error bars represent statistical uncertainty approximated to a Poisson process for the coincidence count uncertainty.

Energy cuts selecting events with neutron energy losses between 0.65MeV to 6.6MeV in the sensitive volume of the detectors were applied in accordance with those adopted in Ref. **[*5*]**. With detector count rates of around 1 kHz, there was not a significant pileup of fission events. Therefore, no correction was applied to the simulation results to compensate for such effects.

a)

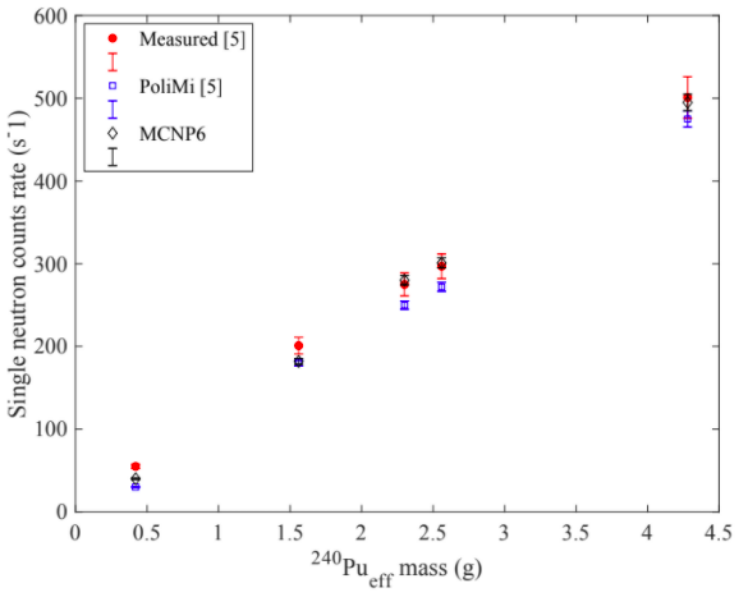

doi:10.7290/ijns070104

b)

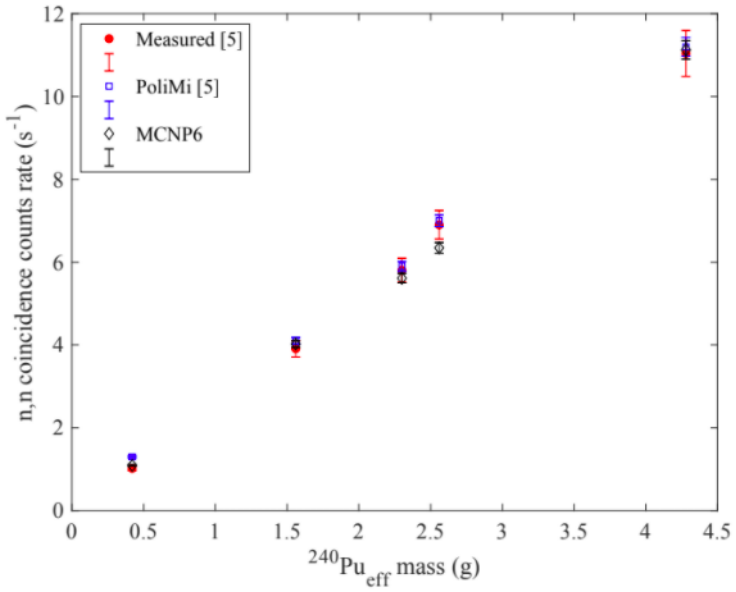

Figure 2: Single-neutron (a) and nn coincidence (b) rates as function of 240Pueff mass for experiment 1. The experimental data and MCNPX PoliMi simulations are taken from Dolan et al. [*5*].

The measurements and MCNP simulations are in quite good agreement for both the single-neutron and nn coincidence count rates in this case. However, the MCNP6 simulation performed somewhat better than MCNP-PoliMi for coincidence events. It is important to note that there are expected differences between the simulation and the experimental data due to certain experimental factors which are not taken into account by the simulation code, such as the non-uniform light collection in the scintillators and the mis-classification of particles in the PSD selection. As discussed in Ref. **[*5*]**, the rather limited discrepancies between the experiment and the simulation could be explained by experimental limitations rather than the simulation parameters and physics description.

Table 1 presents the comparison between the experimental results and the MCNP6 simulations in numerical form. The difference between measured and simulated nn coincidence rates were found to be between 11% and 4% **[*5*]**. Differences of similar magnitude were reported in the comparison with MCNP PoliMi simulations by Dolan et al. **[*5*]**, presenting a maximum of 13% difference for the smaller sample, number 1. The single neutron rates presented smaller differences, ranging from 2% to 8%.

doi:10.7290/ijns070104

Table 1. Ratios of single-neutron and nn rates obtained in experiment* [5], *relative to values calculated using MCNP6.

	Ratio (Measured [5]/MCNP6)	
Sample ID	single n	nn coincidences
1	1,03±0.010	0,89±0.008
3	1,08±0.010	0,90±0.009
4	0,95±0.009	0,93±0.009
2 +3	0,97±0.009	0,96±0.009
1+3+4 *	1,02±0.010	0,96±0.008

In Ref.* **[5] *this point is presented as a sum of samples 1,2 and 3 but the total 240Pu mass doesn't match. The correct mix of samples for this point seems to be 1,3 and 4 according to the total mass reported.*

B. Neutron-Neutron and Gamma-Neutron Coincidence Count Rates

Gamma-neutron coincidences counting rates were calculated and compared with the neutron-neutron rates. Figure 3 presents gn and nn coincidence counting rates as a function of Pu-240 effective mass for the five samples.

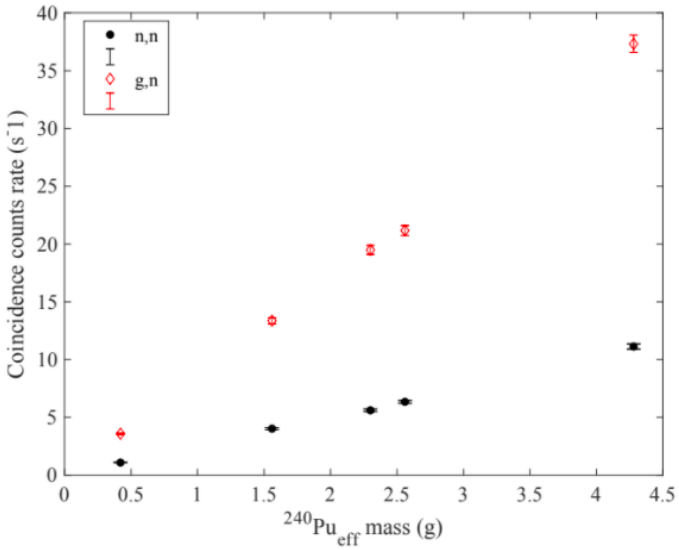

Figure 3: MCNP6 calculated neutron-neutron and gamma-neutron coincidence rates as function of $^{240}Pu_{eff}$ mass.

doi:10.7290/ijns070104

International Journal of Nuclear Security, Vol. 7, No. 1, 2021

As shown in Figure 3, the gn coincidence rate is a more sensitive measure of the Pu-240 effective mass than the nn coincidences without shielding. The difference is approximately a factor of 4, as calculated by the slope of the coincidence rates as a function of Pu-240 effective mass. The high sensitivity of the proposed methodology opens possibilities to investigate the application of the method in SNM pedestrian monitors, where detection in order of a few grams is necessary **[*28*]**.

C. Impact of Shielding on gn Coincidence Rates

In order to address possible applications of the method, we have performed MCNP6 simulations for the setup presented in Ref. **[*5*]** with different shielding configurations, considering the largest Pu-240 sample presented. A broader range of thicknesses, 1 to 7 cm of lead, polystyrene and water shielding, respectively, were applied. The setup design chosen imposed the limit on the thickness range. Dolan et al. **[*5*]** made use of lead shielding of 1 cm thickness to decrease the gamma-ray flux reaching the detectors, and explains the rate of photon/neutron misclassification in the experiment. They reported a decrease of 20% in the neutron doubles detection rate, calculated by MCNPX-PoliMi simulations when such shielding was applied, compared to when no shielding was present.

Despite the fact that lead shielding affects the gn coincidence rates much more than the nn coincidence rates (as expected, since the cross section to gammas in lead is higher than for neutrons), for small thicknesses (less than 4 cm), the rate of gn coincidence is still greater than the nn coincidence rate. From 4 cm of lead and beyond, the attenuation suffered by the gn rate is enough to reduce it to the same level as the nn rate, as can be seen in Figure 4a. Due to the high quantity of hydrogen, water, and polystyrene shielding reduce the nn coincidence rate much more than the gn rate (see Figures 4b and c), hence the predicted gn coincidence rates remain higher until the thickness limit studied – 7 cm.

Figure 5 presents the normalized attenuation of gn coincidence rates calculated with MCNP6 for the three types of shielding studied. The calculations indicate that 50% of attenuation on the detection of gn coincidences is achieved for 1.5 cm of lead, 2.5 cm of polystyrene and 5 cm of water, respectively.

a)

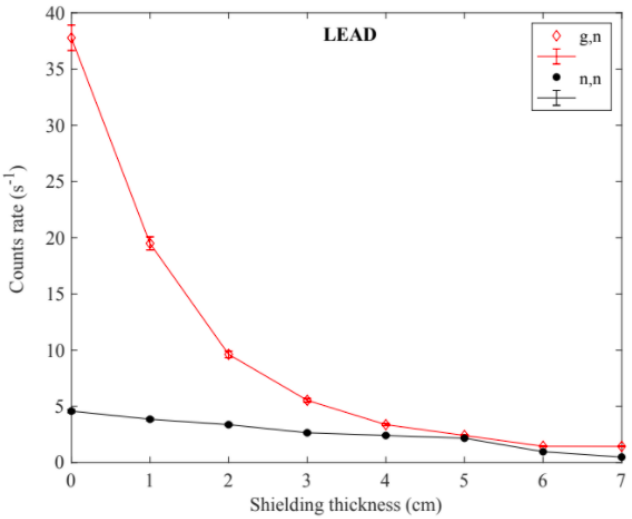

doi:10.7290/ijns070104

b)

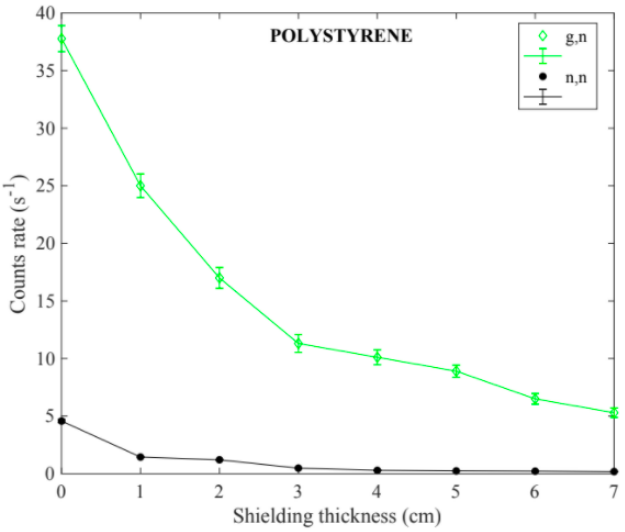

c)

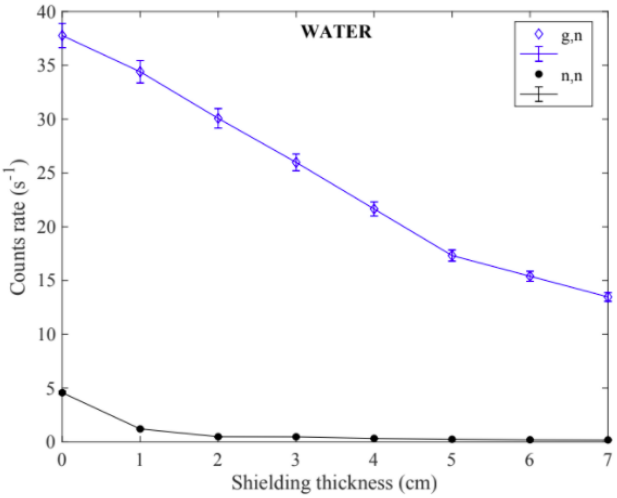

Figure 4: MCNP6 calculated neutron-neutron and gamma-neutron coincidence rates for (a) lead, (b) polystyrene and (c) water shielding as a function of shielding thickness.

doi:10.7290/ijns070104

International Journal of Nuclear Security, Vol. 7, No. 1, 2021

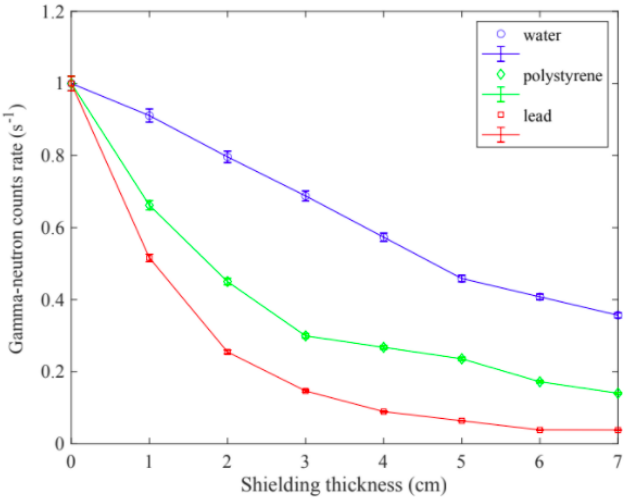

Figure 5: Normalized attenuation from MCNP6 calculated gamma-neutron coincidence rates as function of water, polystyrene, and lead shielding.

IV. Conclusion

In this study, we performed Monte Carlo simulations for prompt nn and gn coincidence counting using liquid organic scintillator detectors in the presence of plutonium samples with varying amounts of shielding, focusing on applications in special nuclear material detection. To investigate the proposed technique for realistic conditions in different applications, we adopted a new Monte Carlo simulation approach that makes use of the MCNP code in its version 6 and the PTRAC card for calculating particle coincidences rates on an event-by-event basis. The MCNP6 simulations were in good agreement with the experimental results presented by Dolan et al. **[*5*]**, with a maximum difference of 11% for the nn coincidence rates. Equivalency was also found between the MCNP6 performed in the present work and the MCNPX PoliMi simulations reported earlier **[*5*]**, indicating that MCNP6 is comparable to the MCNP-PoliMi code in these conditions when it makes use of the PTRAC card.

The results confirm that gamma-neutron coincidence counting results have significantly higher sensitivity to small amounts of SNM (as measured by the Pu-240 effective mass of the samples) than neutron-neutron coincidence counting without the presence of shielding **[*19*]**. The high multiplicity and the short time-of-flight of gamma-rays make the detection of gn coincidences more abundant than nn coincidences when no shielding is present. The same applies to cases with moderate amounts of lead or water shielding. Notably, a 4 cm thick layer of lead shielding is required to attenuate the gn coincidence rate down to the same level as the nn coincidence rate, whereas water and polyestyrene shielding increases the relative efficiency of gn coincidence counting compared with nn counting.

These features are particularly advantageous for pedestrian RPM systems where neutron sensitivity test standards require the use of polyethylene shielding, whereas any metallic shielding is typically detected by other means, as X-ray machines. Further investigation on the use of fast gn coincidence counting as a means to detect SNM in RPM applications was performed by simulations and experiments **[*29*]** following the standard ANSI N42.35-2016 **[*30*]**. It was shown that implementing the fast gn coincidence technique in addition to the standard single gamma and neutron counting improves the sensitivity of the system, making it possible to establish lower alarm thresholds and enabling lower false alarm rates.

The direct detection of the fast neutrons emitted from SNM and preserving the information on their direction and energy also enable imaging capabilities that are being investigated by our group.

doi:10.7290/ijns070104

Other applications in nuclear safeguards, such as spent fuel verification, are also under investigation using Monte Carlo simulations and measurements.

V. Acknowledgements

This research was funded by the Swedish Radiation Safety Authority (SSM) under contract No SSM2016-3954.

VI. Works Cited

1. S. M. Robinson, R. C. Runkle, R. J. Newby, A comparison of performance between organic scintillation crystals and moderated 3He-based detectors for fission neutron detection. *Nucl. Instrum. Methods Phys. Res. Sect. Accel. Spectrometers Detect. Assoc. Equip.* **652**, 404–407 (2011).

2. A. C. Kaplan, M. Flaska, A. Enqvist, J. L. Dolan, S. A. Pozzi, EJ-309 pulse shape discrimination performance with a high gamma-ray-to-neutron ratio and low threshold. *Nucl. Instrum. Methods Phys. Res. Sect. Accel. Spectrometers Detect. Assoc. Equip.* **729**, 463–468 (2013).

3. M. G. Paff, M. Monterial, P. Marleau, S. Kiff, A. Nowack, S. D. Clarke, S. A. Pozzi, Gamma/neutron time-correlation for special nuclear material detection – Active stimulation of highly enriched uranium. *Ann. Nucl. Energy*. **72**, 358–366 (2014).

4. M. G. Paff, M. L. Ruch, A. Poitrasson-Riviere, A. Sagadevan, S. D. Clarke, S. Pozzi, Organic liquid scintillation detectors for on-the-fly neutron/gamma alarming and radionuclide identification in a pedestrian radiation portal monitor. *Nucl. Instrum. Methods Phys. Res. Sect. Accel. Spectrometers Detect. Assoc. Equip.* **789**, 16–27 (2015).

5. J. L. Dolan, M. Flaska, A. Poitrasson-Riviere, A. Enqvist, P. Peerani, D. L. Chichester, S. A. Pozzi, Plutonium measurements with a fast-neutron multiplicity counter for nuclear safeguards applications. *Nucl. Instrum. Methods Phys. Res. Sect. Accel. Spectrometers Detect. Assoc. Equip.* **763**, 565–574 (2014).

6. M. M. Pickrell, A. D. Lavietes, V. Gavron, D. Henzlova, H. Menlove, M. J. Joyce, R. T. Kouzes, The IAEA Workshop on Requirements and Potential Technologies for Replacement of 3He Detectors in IAEA Safeguards Applications. *J. Nucl. Mater. Manag.* **41** (2013) (available at https://resources.inmm.org/jnmm/iaea-workshop-requirements-and-potential-technologies-replacement-3he-detectors-iaea).

7. D. G. Langner, J. E. Stewart, M. M. Pickrell, M. S. Krick, N. Ensslin, W. C. Harker, "Application Guide to Neutron Multiplicity Counting" (LA-13422-M ON:DE00001679, Los Alamos National Laboratory, United States, 1998), doi:10.2172/1679.

8. H. O. Menlove, J. E. Swansen, A High-Performance Neutron Time Correlation Counter. *Nucl. Technol.* **71**, 497–505 (1985).

9. A. Enqvist, C. C. Lawrence, B. M. Wieger, S. A. Pozzi, T. N. Massey, Neutron light output response and resolution functions in EJ-309 liquid scintillation detectors. *Nucl. Instrum. Methods Phys. Res. Sect. Accel. Spectrometers Detect. Assoc. Equip.* **715**, 79–86 (2013).

10. S. Lemaire, P. Talou, T. Kawano, M. B. Chadwick, D. G. Madland, Monte Carlo approach to sequential neutron emission from fission fragments. *Phys. Rev. C*. **72**, 024601 (2005).

doi:10.7290/ijns070104

11. J. H. Hamilton, A. V. Ramayya, S. J. Zhu, G. M. Ter-Akopian, Yu. Ts. Oganessian, J. D. Cole, J. O. Rasmussen, M. A. Stoyer, New insights from studies of spontaneous fission with large detector arrays. *Prog. Part. Nucl. Phys.* **35**, 635–704 (1995).

12. D. L. Bleuel *et al.*, Gamma-ray multiplicity measurement of the spontaneous fission of 252Cf in a segmented HPGe/BGO detector array. *Nucl. Instrum. Methods Phys. Res. Sect. Accel. Spectrometers Detect. Assoc. Equip.* **624**, 691–698 (2010).

13. T. H. Shin, A. D. Fulvio, S. D. Clarke, D. L. Chichester, S. A. Pozzi, (Palm Springs, CA, 2017).

14. S. Li, S. Qiu, Q. Zhang, Y. Huo, H. Lin, Fast-neutron multiplicity analysis based on liquid scintillation. *Appl. Radiat. Isot.* **110**, 53–58 (2016).

15. D. L. Chichester, S. J. Thompson, M. T. Kinlaw, J. T. Johnson, J. L. Dolan, M. Flaska, S. A. Pozzi, Statistical estimation of the performance of a fast-neutron multiplicity system for nuclear material accountancy. *Nucl. Instrum. Methods Phys. Res. Sect. Accel. Spectrometers Detect. Assoc. Equip.* **784**, 448–454 (2015).

16. D. L. Chichester, S. A. Pozzi, J. L. Dolan, M. T. Kinlaw, A. C. Kaplan, M. Flaska, A. Enqvist, J. T. Johnsom, S. M. Watson, "MPACT Fast Neutron Multiplicity System Design Concepts" (INL/EXT-12-27619, Idaho National Laboratory, United States, 2012), doi:10.2172/1057209.

17. A. Enqvist, M. Flaska, S. Pozzi, Measurement and simulation of neutron/gamma-ray cross-correlation functions from spontaneous fission. *Nucl. Instrum. Methods Phys. Res. Sect. Accel. Spectrometers Detect. Assoc. Equip.* **595**, 426–430 (2008).

18. JCC-31™ High Level Neutron Coincidence Counter. *Mirion Technol.*, (available at https://www.mirion.com/products/jcc-31-high-level-neutron-coincidence-counter).

19. D. M. Trombetta, M. Klintefjord, K. Axell, B. Cederwall, Fast neutron- and γ-ray coincidence detection for nuclear security and safeguards applications. *Nucl. Instrum. Methods Phys. Res. Sect. Accel. Spectrometers Detect. Assoc. Equip.* **927**, 119–124 (2019).

20. P. Talou *et al.*, Correlated prompt fission data in transport simulations. *Eur. Phys. J. A.* **54** (2018), doi:10.1140/epja/i2018-12455-0.

21. C. J. Werner, Ed., MCNP User's Manual Code Version 6.2 (2017), (available at https://mcnp.lanl.gov/pdf_files/la-ur-17-29981.pdf).

22. M. E. Rising, "CGMF & FREYA Verification in MCNP6" (LA-UR-16-27710, Los Alamos National Laboratory, 2017), (available at https://mcnp.lanl.gov/pdf_files/la-ur-16-27710.pdf).

23. L. G. Evans, M. A. Schear, J. S. Hendricks, M. T. Swinhoe, S. J. Tobin, S. Croft, A New MCNPX PTRAC Coincidence Capture File Capability: A Tool for Neutron Detector Design, (Los Alamos National Laboratory, Phoenix, AZ, USA, 2011; https://permalink.lanl.gov/object/tr?what=info:lanl-repo/lareport/LA-UR-11-00701).

24. A. C. Kaplan, V. Henzl, H. O. Menlove, M. T. Swinhoe, A. P. Belian, M. Flaska, S. A. Pozzi, Determination of spent nuclear fuel assembly multiplication with the differential die-away self-interrogation instrument. *Nucl. Instrum. Methods Phys. Res. Sect. Accel. Spectrometers Detect. Assoc. Equip.* **757**, 20–27 (2014).

doi:10.7290/ijns070104

25. *MATLAB R2017a* (The MathWorks, Inc.).

26. A. Di Fulvio, T. H. Shin, T. Jordan, C. Sosa, M. L. Ruch, S. D. Clarke, D. L. Chichester, S. A. Pozzi, Passive assay of plutonium metal plates using a fast-neutron multiplicity counter. *Nucl. Instrum. Methods Phys. Res. Sect. Accel. Spectrometers Detect. Assoc. Equip.* **855**, 92–101 (2017).

27. EJ-301, EJ-309 - Neutron/Gamma PSD Liquid Scintillators. *Eljen Technol.*, (available at https://eljentechnology.com/products/liquid-scintillators/ej-301-ej-309).

28. ASTM C1169-97(2012) - Standard Guide for Laboratory Evaluation of Automatic Pedestrian SNM Monitor Performance (2012), (available at https://webstore.ansi.org/standards/astm/astmc1169972012).

29. D. Trombetta, C. Sundaram, K. Axell, B. Cederwall, Sensitive Detection of Special Nuclear Materials for RPM Applications Based on Gamma-Fast Neutron Coincidence Counting (2020), (available at https://conferences.iaea.org/event/181/contributions/15436/attachments/8770/12695/IAEA_202002_v6.pdf).

30. In *ANSI N42.35-2016 (Revision of ANSI N42.35-2006)* (IEEE, 2016; https://ieeexplore.ieee.org/document/7551097).

doi:10.7290/ijns070104